

SUPPLEMENTAL TEXT AND FIGURES

Prrx1 isoform switching regulates pancreatic cancer invasion and metastatic colonization

Shigetsugu Takano, Maximilian Reichert, Basil Bakir, Koushik K. Das, Takahiro Nishida, Masaru Miyazaki, Steffen Heeg, Meredith A. Collins, Benoît Marchand, Philip D. Hicks, Anirban Maitra, and Anil K. Rustgi

Supplemental Figure Legends

Figure S1

(A) Protein domains of PRRX1A and PRRX1B share amino acids 1-199. PRRX1B lacks the OAR (otp, aristaless and rax) domain and has an alternative carboxy (C)-terminus. **(B, C)** Morphological differences between mouse primary pancreatic ductal cells (PDCs) and neoplastic pancreatic cells in 3D culture, including paired primary tumor and liver metastatic cells. **(B)** Representative morphological characteristics of cyst growth (spheroid cyst, irregular cyst and spindle shaped cells) in 3D culture. **(C)** Comparison of respective morphological characteristics. **(D)** Comparisons for percentages of cysts between two primary cancer cell lines (KPC1, KPC2 cells) and matched metastatic cells (KPC1Liv, KPC2Liv2 cells) in 3D culture (n = 4, *p < 0.05, mean ± SEM). **(E, F)** Gene expression profiles of EMT related molecules (*Cdh1*, E-cadherin; *Cdh2*, N-cadherin) (E) and *Prrx1a/Prrx1b* (F) in 6 mouse pancreatic ductal cell lines in 3D culture (n = 5, * p < 0.05, mean ± SEM). **(G)** The ratio of *Prrx1a* to *Prrx1b* gene expression in KPC1 and KPC1Liv cells as well as KPC2 and KPC2Liv2 cells (n = 5, *p < 0.05, mean ± SEM). **(H)** Relative gene expression of *Prrx1a* and *Prrx1b* in isoform specific overexpressing cell lines (top panels) or isoform specific siRNA knockdown cell lines (bottom panels) (mean ± SD). **(I)** Western blot analysis for E-CADHERIN in two primary pancreatic cancer cell lines and their respective metastatic cancer cell lines (left panels). E-CADHERIN levels in KPC2Liv2 cells treated with isoform specific Prrx1 siRNAs (right panels). The band

intensities were normalized to β -ACTIN. **(J)** Single cell pancreatosphere formation assays on KPC1 and KPC1Liv cells as well as KPC2 and KPC2Liv2 cells (*p < 0.00001, mean \pm SEM). Statistical analyses were performed using the Mann-Whitney-Wilcoxon test. **(K)** Single cell pancreatosphere assays on isoform-specific knockdown KPC2 cells (*p < .05, **p < 0.0001, mean \pm SEM). **(L)** Model of the relationship between Prrx1a and Prrx1b in EMT-MET plasticity during pancreatic cancer progression.

Figure S2

(A) PRRX1A and **(B)** PRRX1B Immunizing Study. Sections from a PRRX1A-overexpressing tumor or a PRRX1B-overexpressing tumor derived from our orthotopic transplantation model were stained with **(A)** PRRX1A or **(B)** PRRX1B antibody incubated overnight at room temperature with either PBS (1-3) or PRRX1A/1B peptide at a ratio of 1 μ g of antibody to 10 μ g of peptide (4-6). Sections were stained at a concentration of 2.2 μ g/mL of antibody incubated for 2 hours at room temperature. Each original image (top row) was deconvoluted into hematoxylin signal (second row) and antibody signal (bottom row) using the "H&E DAB" deconvolution filter in the FIJI version of ImageJ. As can be observed in both the original image panels (1 compared to 4) and the deconvoluted images of antibody staining (3 compared to 6), the peptide effectively abrogates signal. 10X magnification. **(C)** Representative pictures of IF staining for PRRX1B (red), N-

CADHERIN (NCAD) (cyan), YFP (green) and DAPI (blue) in the invasive regions of KP^{fl}CY tumors. The boxed region is magnified in the right panel. White arrows indicate single invasive cells expressing PRRX1B/N-CADHERIN/YFP. A PRRX1B+/N-CADHERIN+/YFP+ cell is magnified in the inset. Scale bar: 50 μ m. **(D)** Comparison of PRRX1A+/N-CADHERIN+/YFP+ cells and PRRX1B+/N-CADHERIN+/YFP+ to N-CADHERIN+/YFP+ cells in invasive regions of KP^{fl}CY tumors. Number of N-cadherin+/YFP+ cells analyzed as follows: PRRX1A: n = 92, for PRRX1B: n = 86; Welch's t-test, mean \pm SEM.

Figure S3

(A) Cellular morphology of KP^{fl}CY cells cultured on 2D plastic plates. KP^{fl}CY cells are endogenously labeled YFP (small box in right panel). **(B)** Relative gene expression of *Prrx1a* and *Prrx1b* in isoform specific overexpressing KP^{fl}CY cells. (mean \pm SD) **(C)** IF staining for PRRX1B (red), YFP (green) and DAPI (blue) in KP^{fl}CY control tumors obtained by orthotopic transplantation of KP^{fl}CY cells. PRRX1B is strongly expressed in disseminating cancer cells at the invasive front of tumors. All scale bars: 50 μ m.

Figure S4

(A) Representative histology of primary PDAC in KPC2 control, KPC2-Prrx1a and

KPC2-Prrx1b tumors in orthotopic transplantation models. Scale bar: 50 μm . **(B)** Demonstrative photographs for intra-portal vein injection model. Left panel: A view during the procedure. White arrows indicate portal vein and pancreas, respectively. Right panel: Fourteen days after injection of cancer cells. White arrows show liver metastases. **(C)** *In vitro* proliferation assays with knockdown of Prrx1 isoforms using isoform specific siRNAs in KPC2Liv2 metastatic cells. Knockdown of Prrx1a significantly impairs cell proliferation compared to control or Prrx1b knockdown in metastatic cells (mean \pm SD, * $p < 0.01$). **(D)** Primary tumor volume and frequency of liver metastasis in orthotopic transplantation model using KPC2 control cells. Upper panel: schematic of experimental design. (8 time points, each $n = 4$). Lower panels: primary tumor volume (left) (mean \pm SEM) and frequency of liver metastasis (right). **(E)** Gene expression pattern of the two Prrx1 isoforms 24 hours after +/- doxycycline treatment (mean \pm SD).

Figure S5

(A) Comparison of relative *Prrx1a* and *Prrx1b* gene expression between KPC2 control and shPrrx1a/b cells in 3D culture (mean \pm SD). **(B)** Morphological differences between KPC2 control and shPrrx1a/b cells in 3D culture. Scale bar: 100 μm . **(C)** Relative gene expression for EMT-related molecules (*Cdh1*, E-cadherin; *Cdh2*, N-cadherin) in 3D culture (mean \pm SD). **(D)** Invasion assays with KPC2 control and shPrrx1a/b cells (mean \pm SEM). **(E)** Percentage of sphere forming cells with

KPC2 control and shPrrx1a/b cells (mean \pm SEM).

Figure S6

(A) IHC analyses for PRRX1A and PRRX1B in primary human PDAC samples (number of samples for PRRX1A, n = 105; for PRRX1B, n = 103; overlapping samples with both PRRX1A and PRRX1B, n = 100; total number of samples, n = 108). **(B)** IHC analyses for PRRX1A and PRRX1B in primary and metastatic human PDAC samples (for primary PDAC, n = 100; for metastatic PDAC, n = 12; paired primary and metastatic PDAC, n = 7). **(C)** IHC analysis of primary human PDAC samples demonstrates PRRX1B staining primarily at the invasive front of tumor tissue (right panel), while PRRX1A expression is present throughout the samples (left panel). **(D)** IHC categories (Low and High) for PRRX1A and PRRX1B in primary and metastatic PDAC. **(E)** Comparison of IHC scores for PRRX1A and PRRX1B between primary and metastatic PDAC in pair-matched samples (n = 7, Welch's t-test).

Figure S7

(A) Relative *mHgf* gene expression in 3D culture in both wild-type and neoplastic primary mouse cell lines (mean \pm SD). **(B)** Relative gene expression for the two *Prrx1* isoforms and EMT-related markers at indicated times after mouse recombinant HGF

treatment of KPC2 cells (mean \pm SD).

Figure S8

(A) Morphological changes in Panc1 cells 24 hours after treatment with human recombinant HGF (hrHGF) and/or ficlatuzumab (Fic). Scale bar: 20 μ m. **(B)** Invasion assays of Panc1 cells treated with hrHGF and/or Fic. **(C)** Invasion assays of Prrx1b overexpressing Panc1 cells with or without Fic (mean \pm SEM). **(D)** Synergistic effects of gemcitabine treatment and Prrx1b silencing on cell viability in metastatic KPC2Liv2 cells *in vitro* (mean \pm SEM) after 48 hours of treatment.

SUPPLEMENTAL EXPERIMENTAL PROCEDURES

Invasion assay

Mouse cancer cell cells were plated onto BD BioCoat Matrigel Invasion Chambers (8 μ m pore size) (BD Biosciences, Bedford, MA) at a concentration of 4×10^5 cells/ml in Dulbecco Modified Eagle Medium (DMEM) (Sigma Chemical Co, St Louis, MO) supplemented with 0.5% fetal bovine serum (FBS). DMEM supplemented with 10% FBS or 10ng/ml mouse recombinant HGF (#2207-HG, R&D systems) served as the chemoattractant in the lower chamber. For human HGF-inhibition experiments, 10ng/ml human recombinant HGF (#294-HG, R&D systems) and 20mg/ml of the neutralizing human HGF antibody ficlatuzumab (AV-299; SCH 900105; AVEO Pharmaceuticals) were used. Panc1 cells were pre-treated for 1 hour before being dissociated and plated at a density of 1×10^5 cells/well. Invading cells were stained by Calcein AM fluorescent dye (BD Biosciences, Bedford, MA) according to the manufacturer's instructions. Quantification was performed in a blinded fashion through manual counting of four high-power fields per well. Each experiment was performed independently in quadruplicate at least three times. $P < 0.05$ was statistically significant (Mann-Whitney-Wilcoxon test). Error bars represent the standard error of the mean (SEM).

Single-cell pancreatosphere assay

Single cells were sorted by FACS (FACSDiva flowcytometer and software, BD Bioscience, Bedford, MA) and directly plated in Costar ultralow-attachment 96-well plates (Corning Incorporated, NY) with one cell per well. After plating cells, the presence of a single cell per well was confirmed by light microscopy. Cells were grown in sphere media as described previously (Reichert, Takano, von Burstin, et al. 2013) with media changes every other day. Sphere formation was analyzed 7 days after plating and photodocumented using the Leica DMIRB Inverted Microscope. Sphere-assays were performed independently at least three times. $P < 0.05$ was statistically significant (Mann-Whitney-Wilcoxon test). Error bars represent the standard error of the mean (SEM).

Western blotting

Western blotting was performed as described previously (Reichert, Takano, von Burstin, et al. 2013). Anti-mouse E-cadherin antibody (610182, dilution 1:3000, BD Biosciences) and anti-mouse β -actin (A5316, dilution 1:5000, Sigma-Aldrich) antibody were used for detection. Western blots were quantified by densitometry analysis and normalized to β -actin using the Image J software. Experiments were performed in triplicate. Error bars represent the standard error of the mean (SEM).

Immunohistochemical and immunofluorescence staining

Custom rabbit anti-PRRX1A and anti-PRRX1B antibodies were generated by Pacific Immunology Corporation (Ramona, CA). In addition, the following commercially available antibodies were used: anti-GFP (ab13970, dilution 1:1000, Abcam, Cambridge, MA), anti-mouse E-cadherin (#610182, dilution 1:500, BD Biosciences, Bedford, MA), anti-mouse N-cadherin (#610921, dilution 1:200, BD Biosciences), anti-mouse HGF (AF2207, dilution 1:200, R&D systems), and anti-human HGF (AF294-NA, dilution 1:200, R&D systems).

Peptide blocking study

Peptides used for validation of custom PRRX1A and PRRX1B antibodies were obtained from Pacific Immunology Corporation. The peptides used for blocking were identical in sequence to peptides used to immunize rabbits. The sequence for PRRX1A and PRRX1B are as follows: PRRX1A – amino acids 226-240 (NLRLKAKEYSLQRNQ) and PRRX1B – amino acids 200-217 (RSSSLPRCCLHEGLHNGF). Stained slides were imaged and then deconvoluted in ImageJ (FIJI version) using the H&E DAB deconvolution filter.

Table S1: Primers RT-qPCR

<i>mPrrx1a</i>	FW: 5'-ACAGCCTCTCCGTACAGCGC-3'
	RV: 5'-AGTCTCAGGTTGGCAATGCT-3'
<i>mPrrx1b</i>	FW: 5'-CATCGTACCTCGTCCTGCTC-3'

RV: 5'-GCCCCTCGTGTAACAACAT-3'

mCyclophilin FW: 5'-ATGGTCAACCCCACCGTGT-3'

RV: 5'-TTCTGCTGTCTTTGGAACCTTGTGTC-3'

mEcad FW: 5'-TCAAGCTCGCGGATAACCAGAACA-3'

RV: 5'-ATTCCCGCCTTCATGCAGTTGTTG-3'

mSlug FW: 5'-CCACACATTGCCTTGTGTCTGCAA-3'

RV: 5'-TGTGCCCTCAGGTTTGATCTGTCT-3'

mSnail FW: 5'-ACACTGGTGAGAAGCCATTCTCCT-3'

RV: 5'-TCTTCACATCCGAGTGGGTTTGGGA-3'

mNcad FW: 5'-ATGGCCTTTCAAACACAGCCACAG-3'

RV: 5'-ACAATGACGTCCACCCTGTTCTCA-3'

mTwist FW: 5'-AGCTGAGCAAGATTCAGACCCTCA-3'

RV: 5'-TGCAGCTTGCCATCTTGGAGT-3'

mVim (Vimentin) FW: 5'-AAGCACCCCTGCAGTCATTCAGA-3'

RV: 5'-GCAAGGATTCCACTTTCCGTTC-3'

mZeb1 FW: 5'-TGAGCACACAGGTAAGAGGCC-3'

RV: 5'-GGCTTTTCCCCAGAGTGCA-3'

mZeb2 FW: 5'-TGATAGCCTTGCAAACCCTCTGGA-3'

RV: 5'-TCCTTCATTTCTTCTGGACCGGCT-3'

mFN1 (Fibronectin) FW: 5'-ATCACAGTAGTTGCGGCAGGAGAA-3'

RV: 5'-TGTCATAGTCAATGCCAGGCTCCA-3'

mFak

FW: 5'-ACCATCCCTAACCATTGCCGAGAA-3'

RV: 5'-ACTTTGGTATTGATGGCAACGCCC-3'

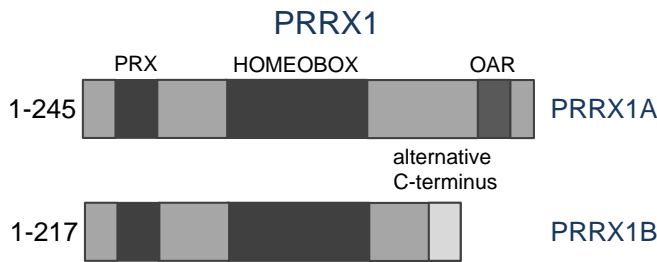
mHgf

FW: 5'-TTGGGATTCGCAGTACCCTCACAA-3'

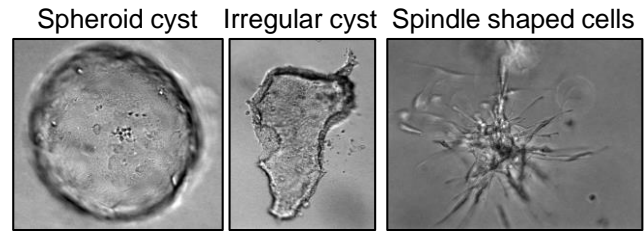
RV: 5'-TAGCCAACCTCGGATGTTTGGGTCA-3'

Figure S1

A



B



Cell Line Nomenclature:

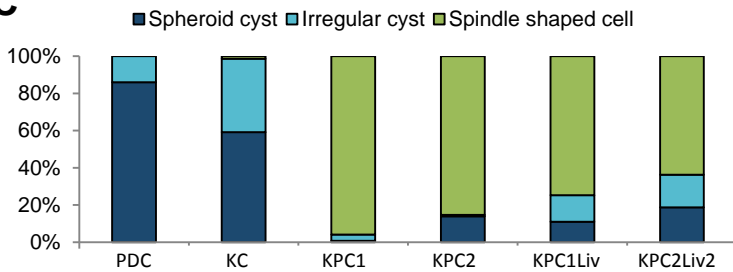
PDC: Normal pancreatic ductal cells

KC: *Pdx1-cre; LSL-Kras^{G12D/+}* (PanIN cells)

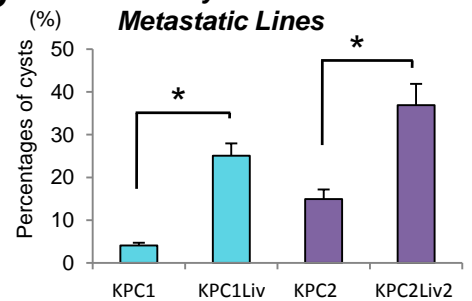
KPC1, KPC2: *Pdx1-cre; LSL-Kras^{G12D/+}; p53^{R172H/+}* (Cancer cells)

KPC1Liv, KPC2Liv2: Liver metastatic cells derived from KPC1 and KPC2 tumors

C Cyst Formation in 3D Culture of Pancreatic Cell Lines



D Cyst Formation in 3D Culture of Primary Tumor and Paired Metastatic Lines



E

Gene Expression Profiles of Pancreatic Cell Lines

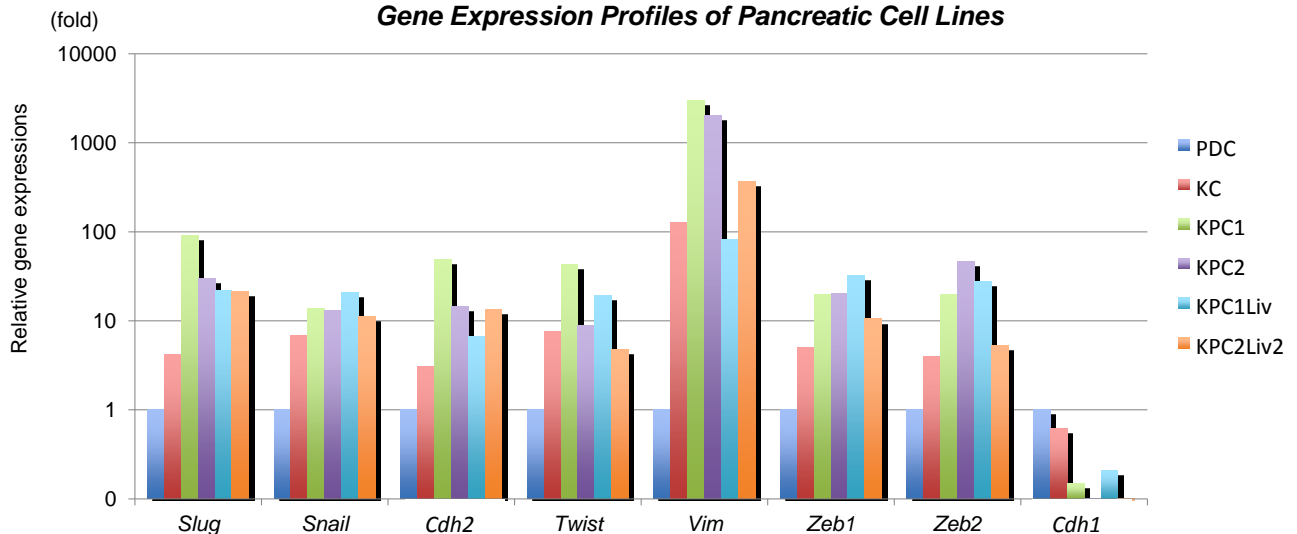
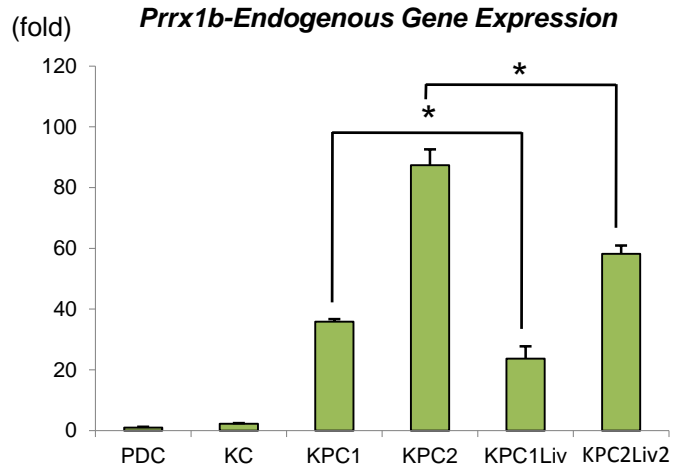
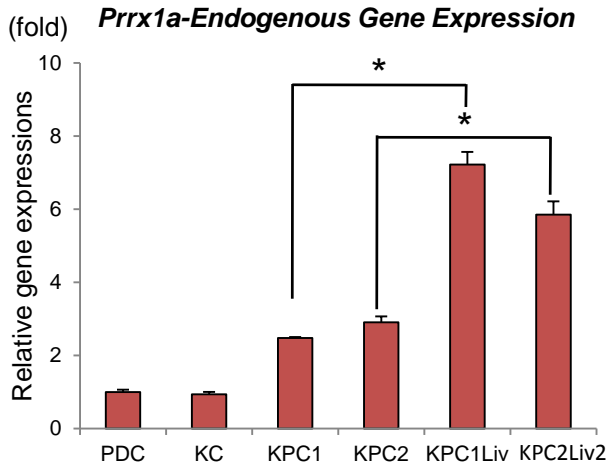


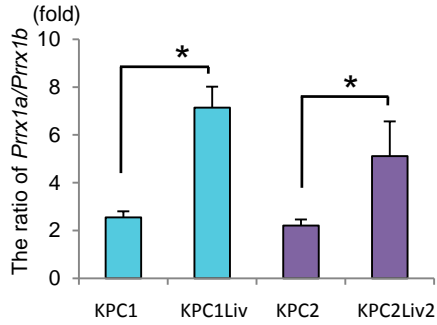
Figure S1

F

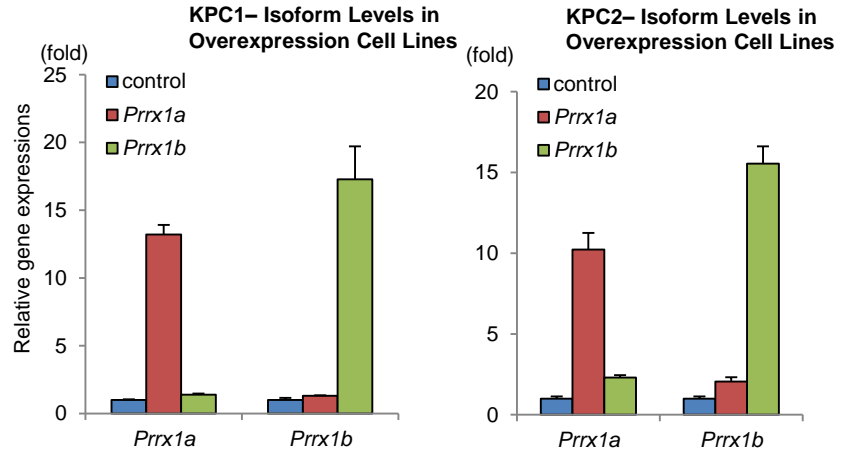


G

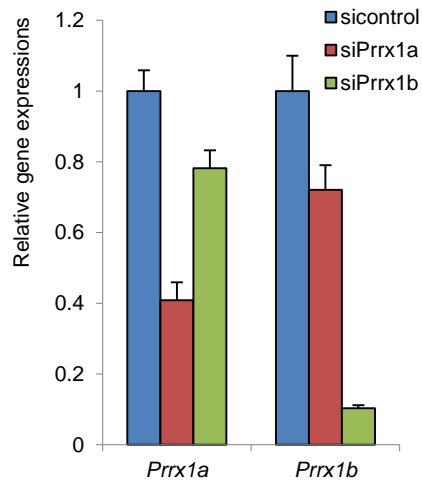
Relative Endogenous *Prrx1a*/*Prrx1b* Gene Expression Ratios



H



KPC1 - Isoform Levels in Knockdown Cell Lines



KPC2 - Isoform Levels in Knockdown Cell Lines

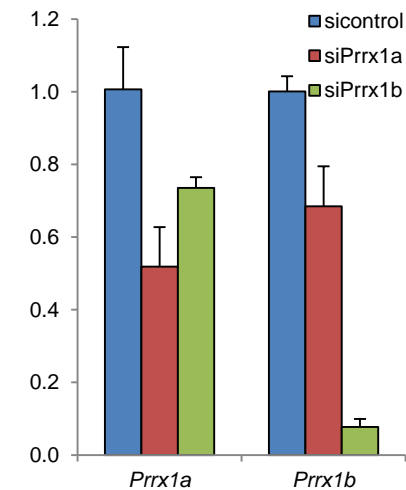
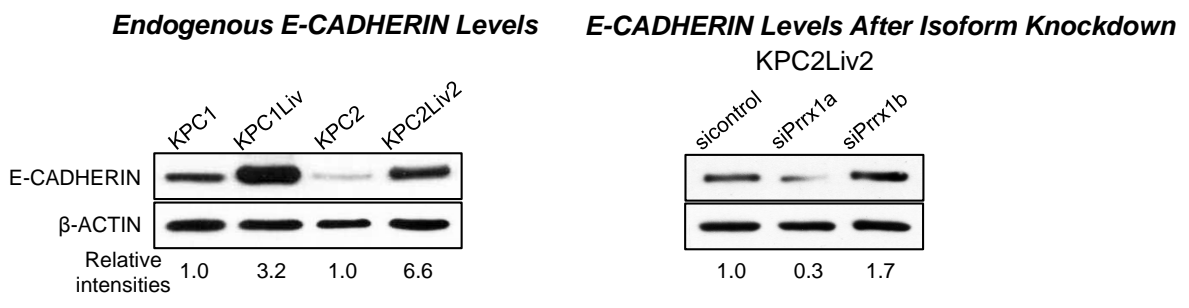
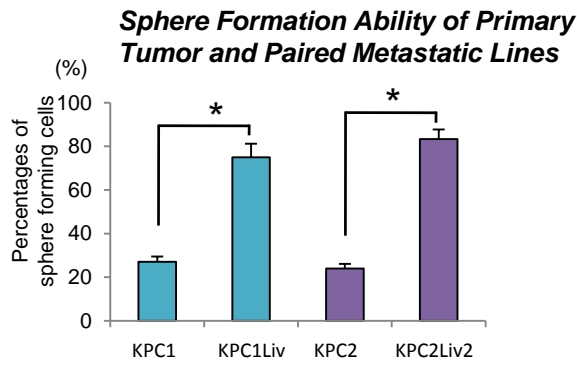


Figure S1

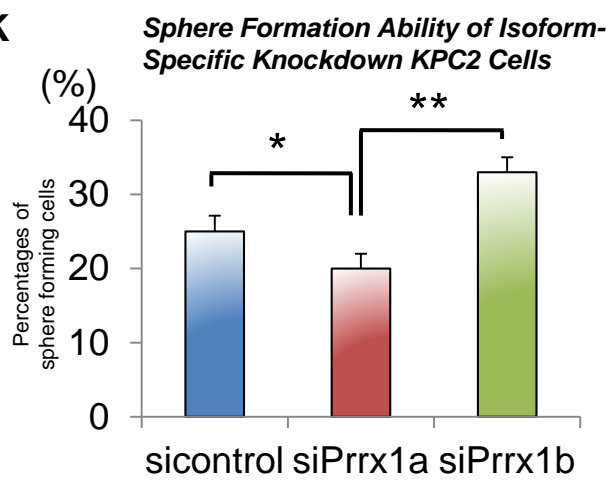
I



J



K



L

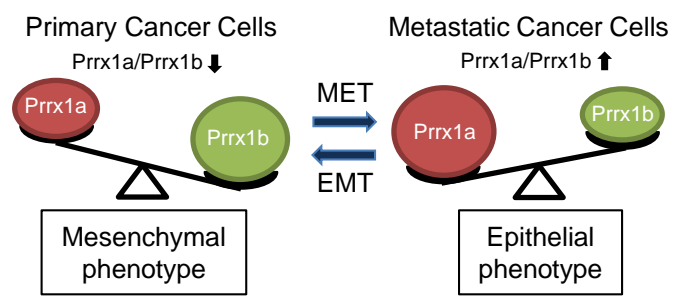
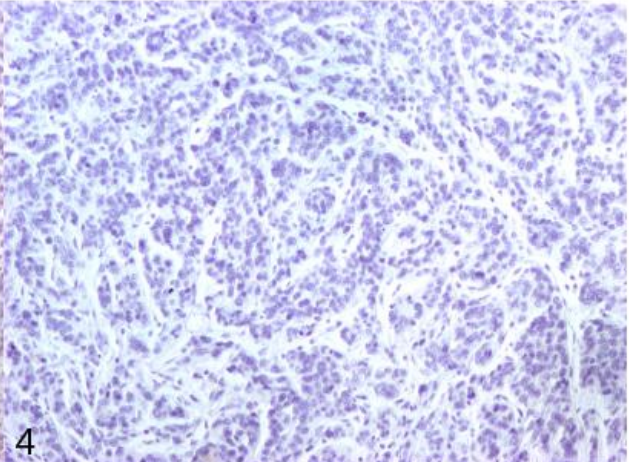
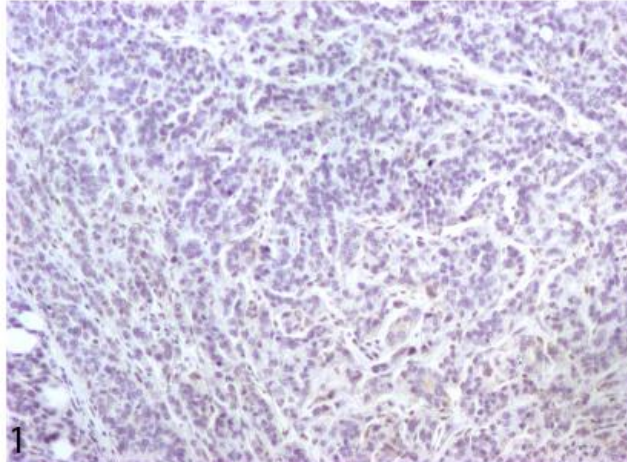


Figure S2A

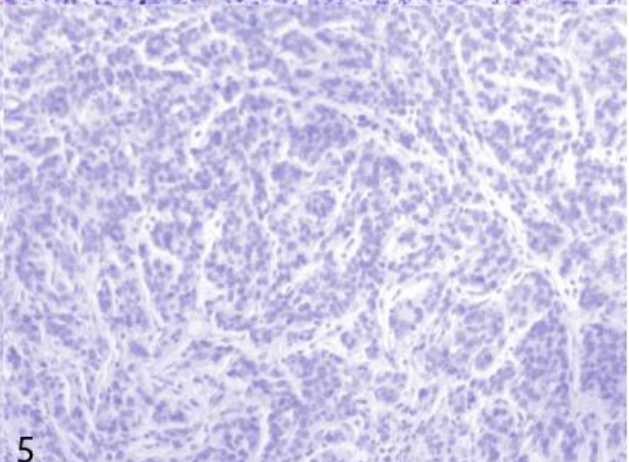
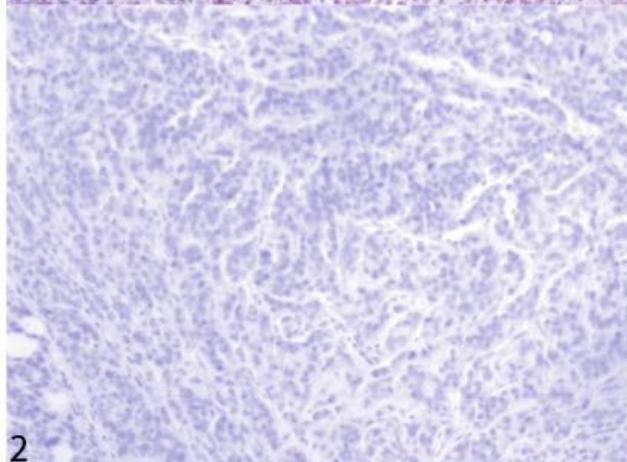
PRRX1A Antibody Incubated with PBS PRRX1A Antibody Incubated with Peptide

10X Magnification

Original Image



Hematoxylin Signal



Antibody Signal

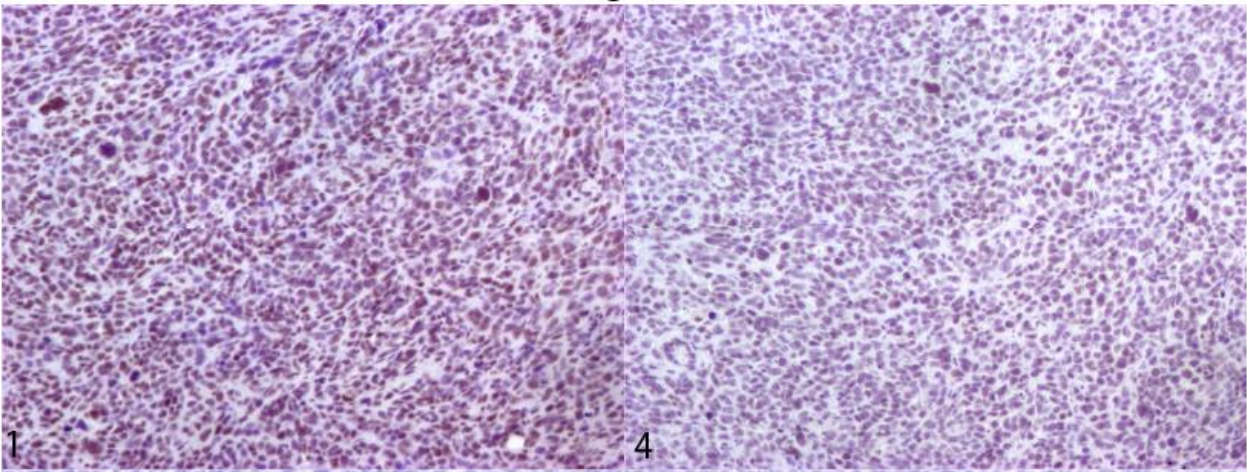


Figure S2B

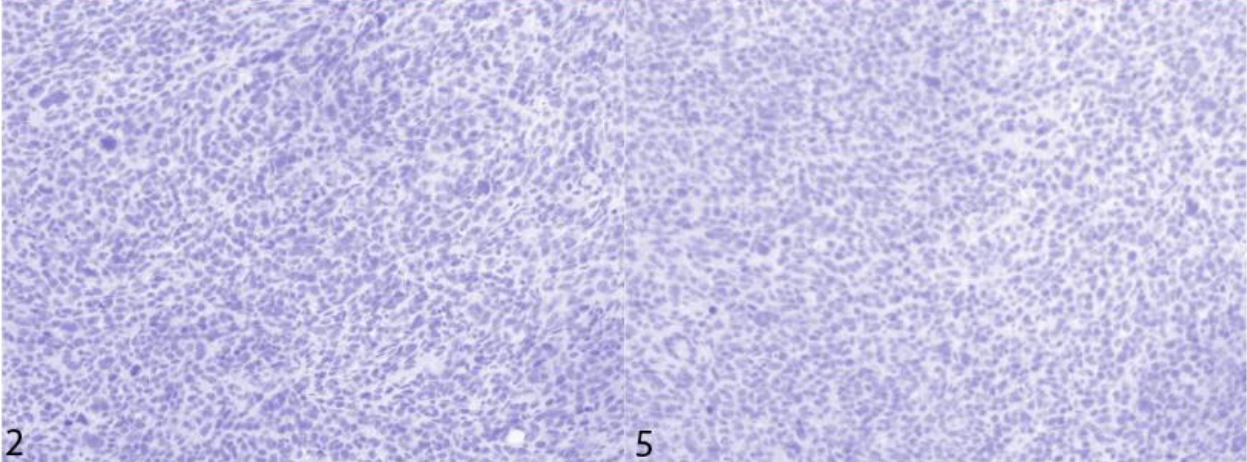
PRRX1B Antibody Incubated with PBS PRRX1B Antibody Incubated with Peptide

10X Magnification

Original Image



Hematoxylin Signal



Antibody Signal

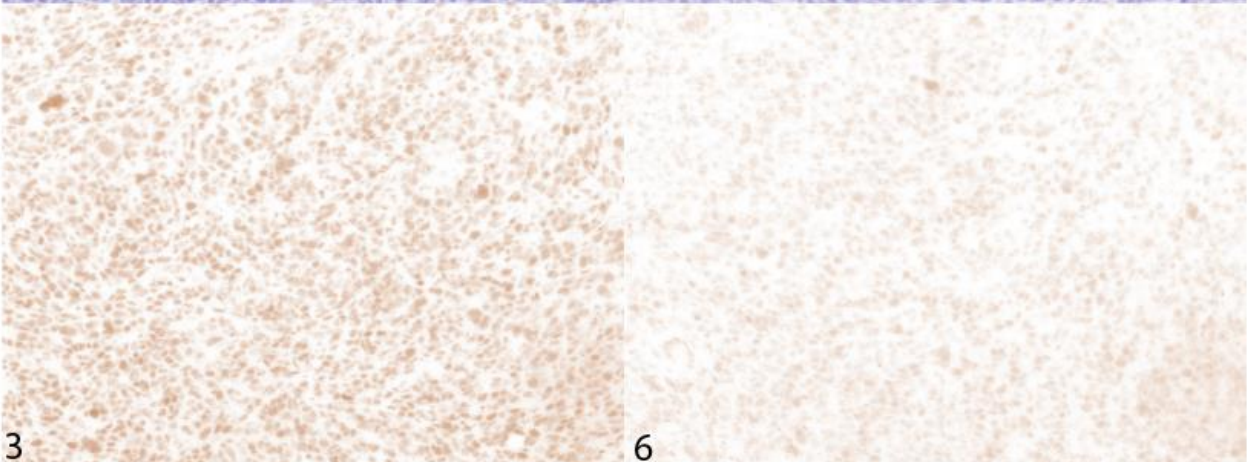
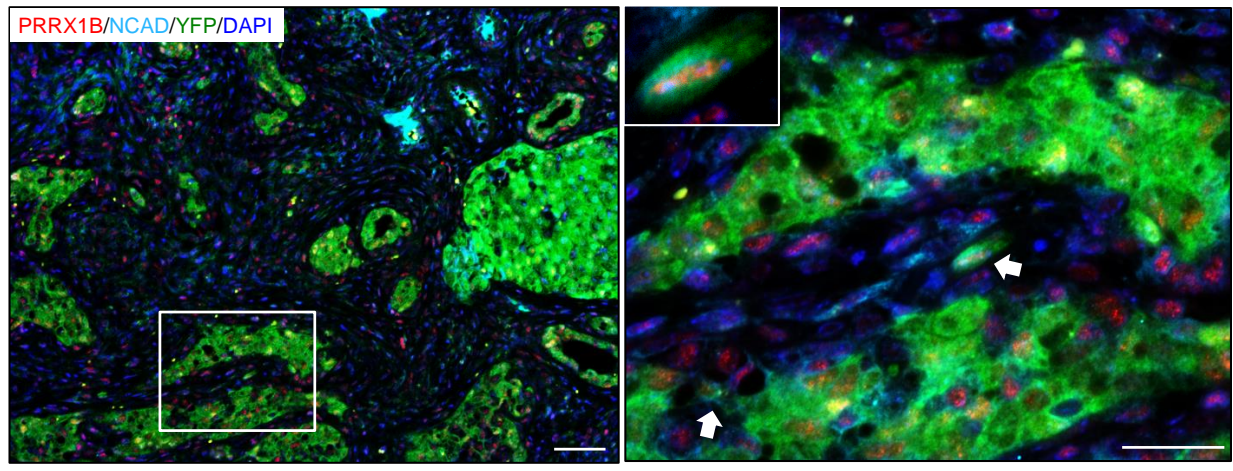


Figure S2

C



D

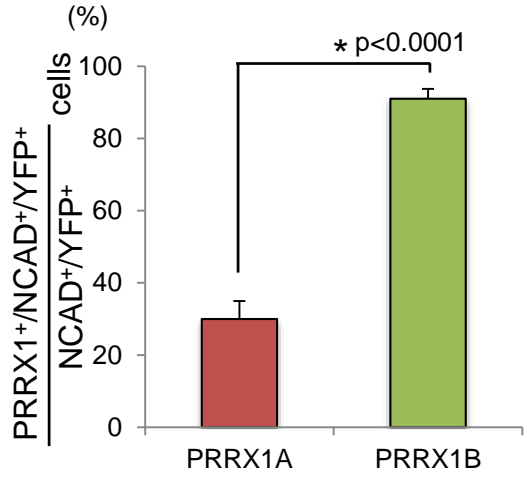
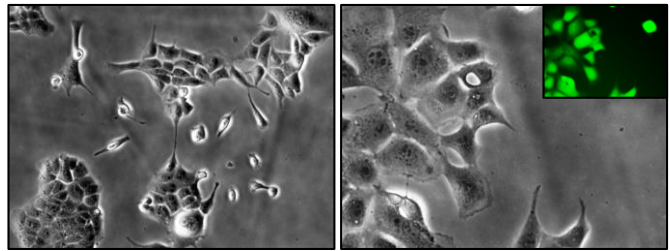
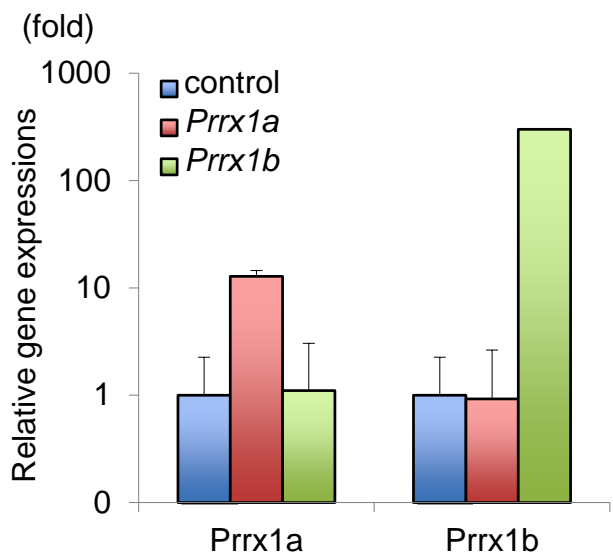


Figure S3

A



B KP^{fl}CY – Isoform Specific Overexpression Levels



C

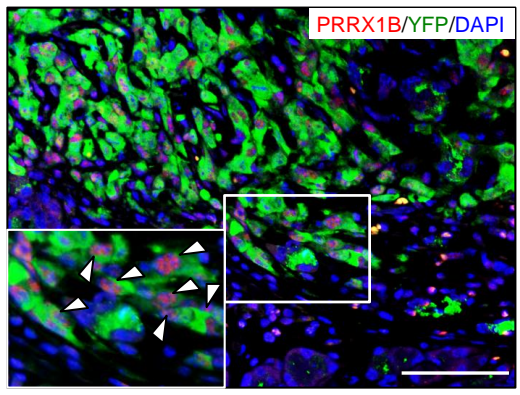


Figure S4

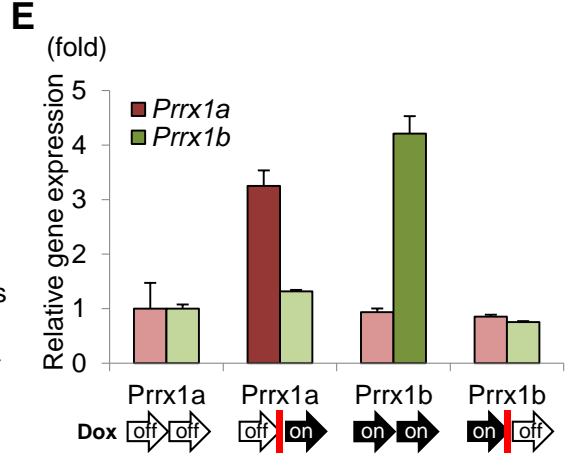
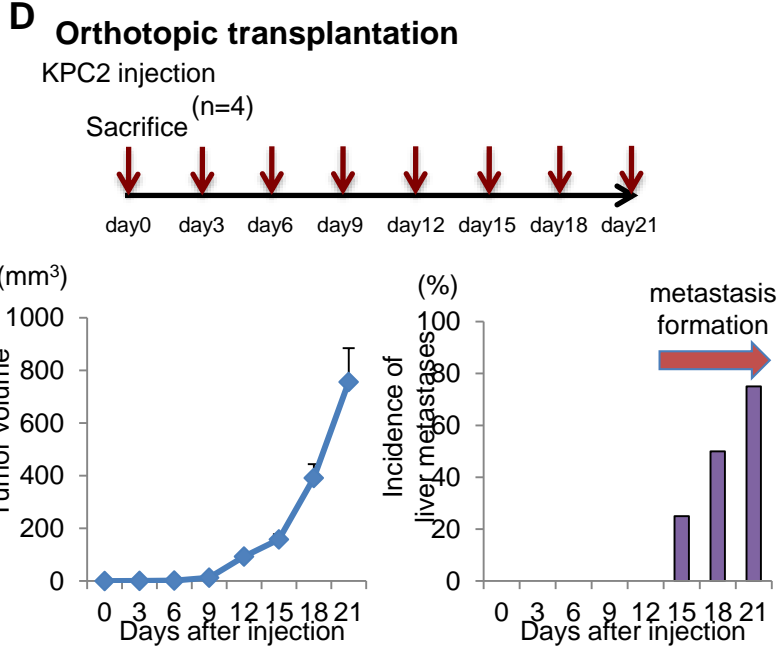
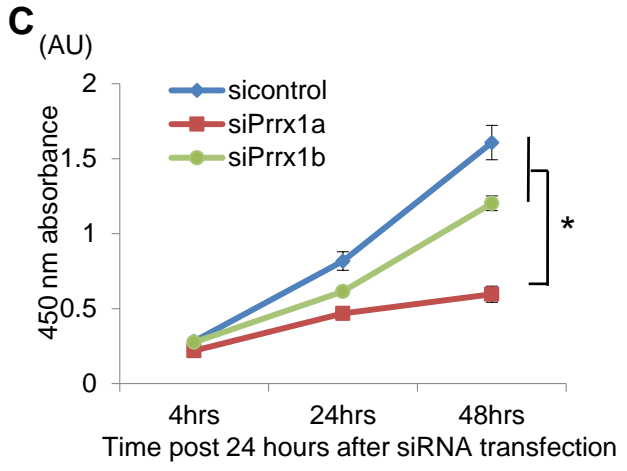
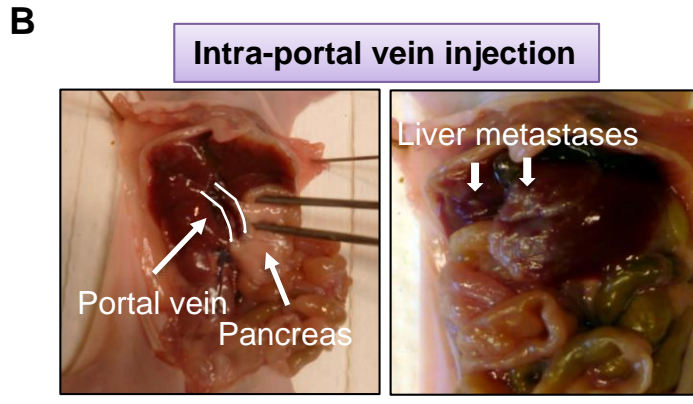
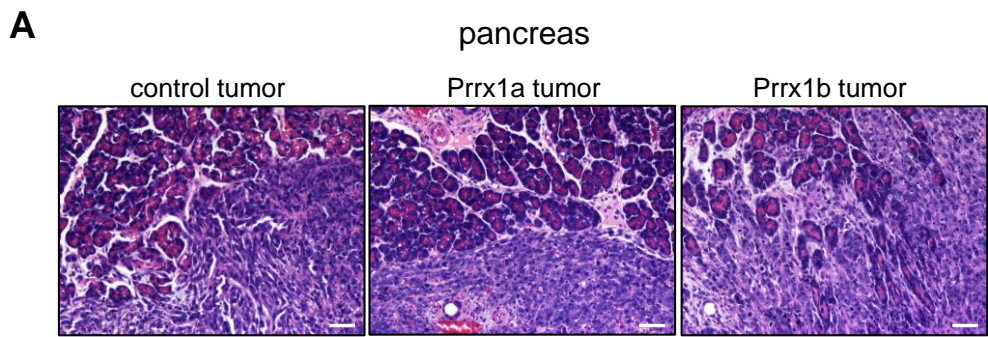


Figure S5

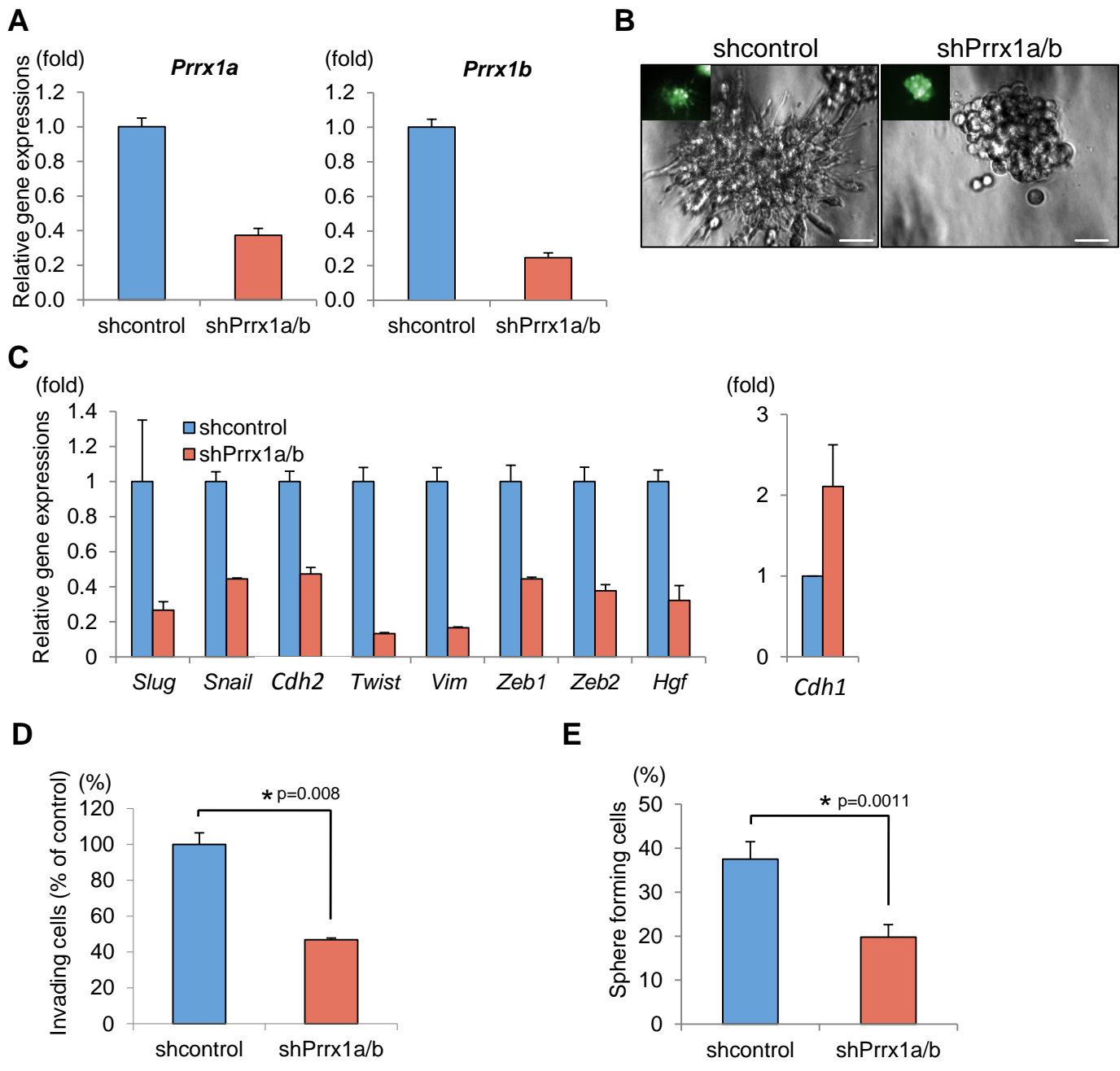
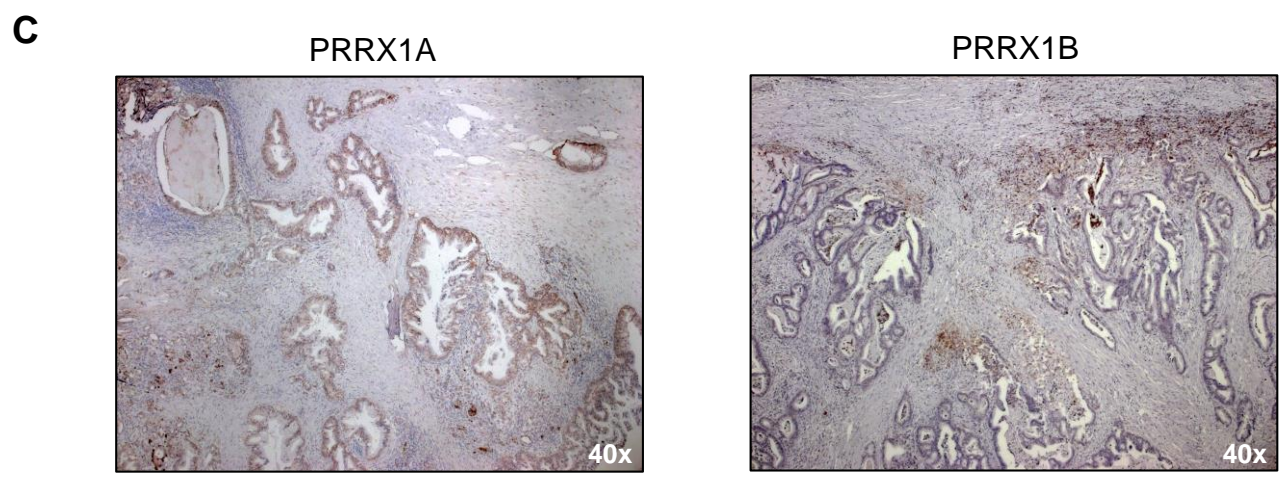
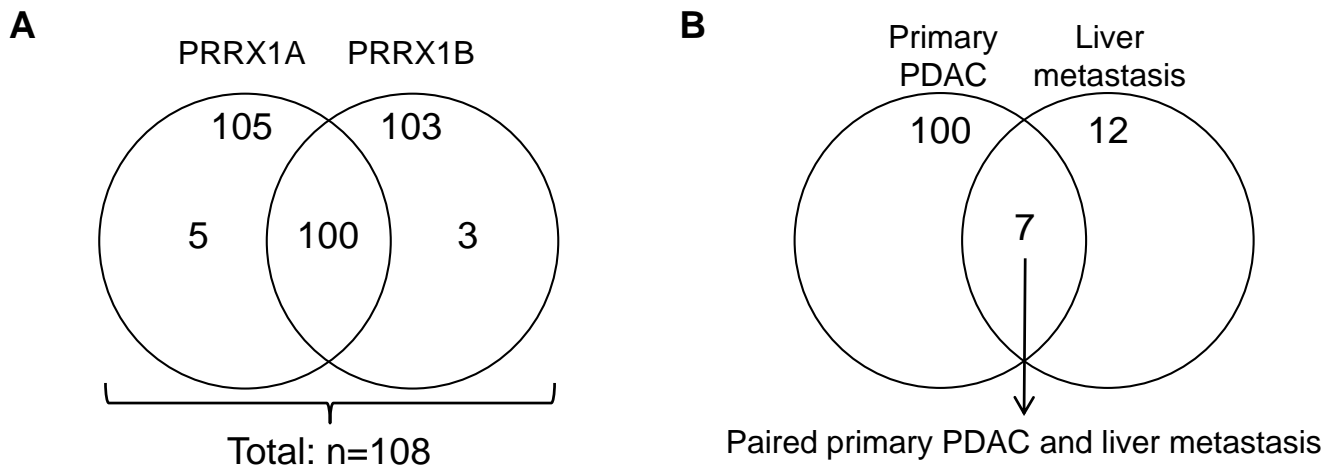


Figure S6



D

Primary PDAC			Liver metastasis		
PRRX1A (n=105)	Low (n=53)	High (n=52)	PRRX1A (n=12)	Low (n=2)	High (n=10)
PRRX1B (n=103)	Low (n=56)	High (n=47)	PRRX1B (n=12)	Low (n=7)	High (n=5)

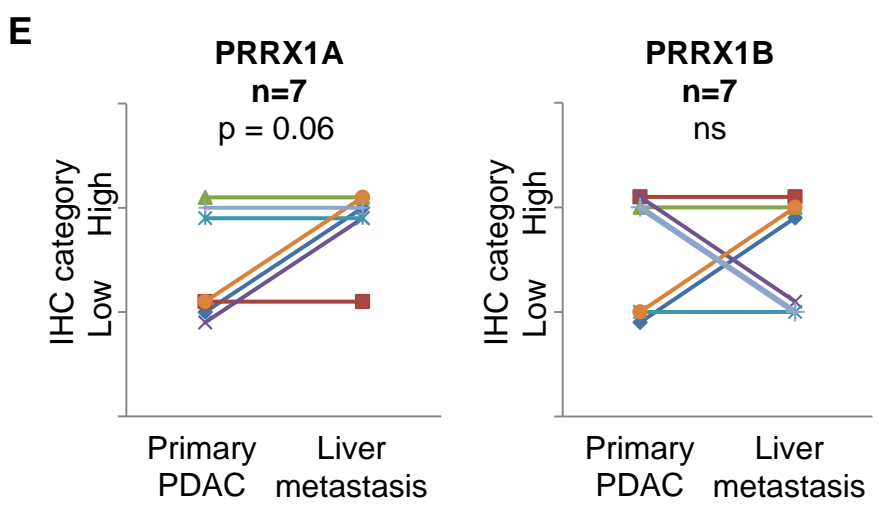


Figure S7

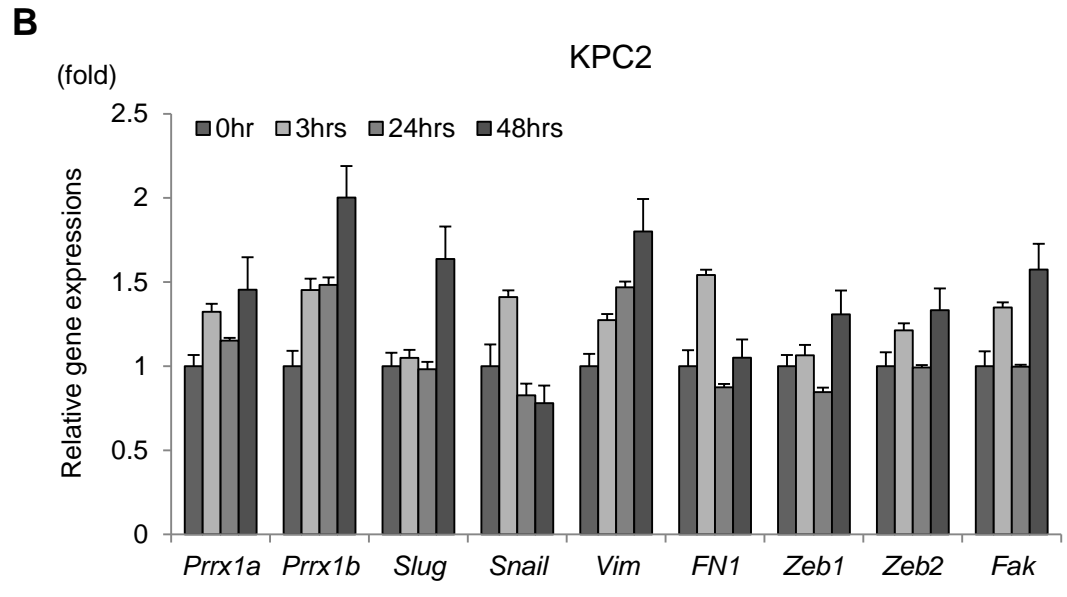
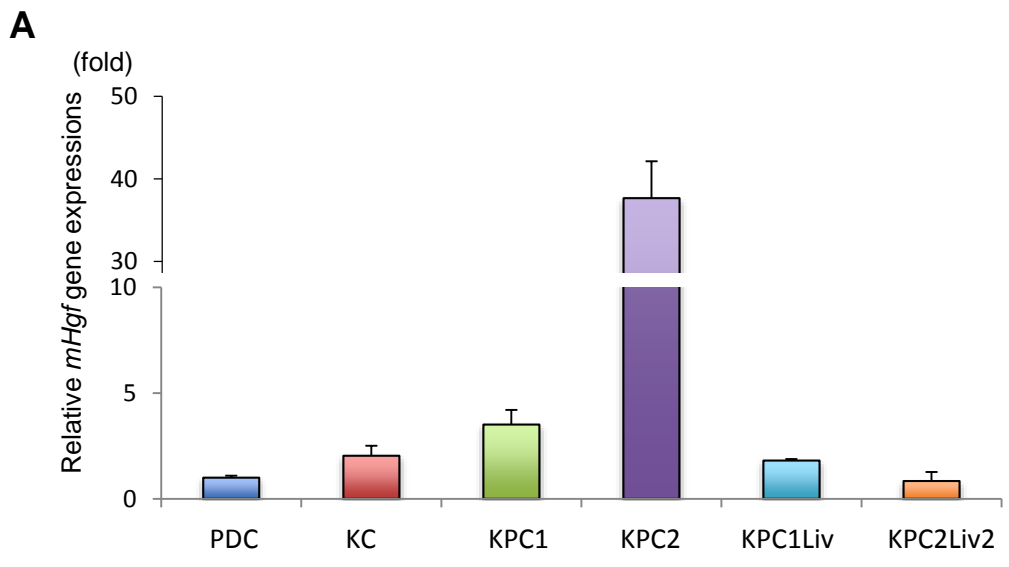


Figure S8

